

## *Retraction*

# **Retracted: Color Image Landscape Photo Hand-Painted Effect Evaluation with PFA Algorithm**

### **Advances in Multimedia**

Received 3 October 2023; Accepted 3 October 2023; Published 4 October 2023

Copyright © 2023 Advances in Multimedia. This is an open access article distributed under the Creative Commons Attribution License, which permits unrestricted use, distribution, and reproduction in any medium, provided the original work is properly cited.

This article has been retracted by Hindawi following an investigation undertaken by the publisher [1]. This investigation has uncovered evidence of one or more of the following indicators of systematic manipulation of the publication process:

- (1) Discrepancies in scope
- (2) Discrepancies in the description of the research reported
- (3) Discrepancies between the availability of data and the research described
- (4) Inappropriate citations
- (5) Incoherent, meaningless and/or irrelevant content included in the article
- (6) Peer-review manipulation

The presence of these indicators undermines our confidence in the integrity of the article's content and we cannot, therefore, vouch for its reliability. Please note that this notice is intended solely to alert readers that the content of this article is unreliable. We have not investigated whether authors were aware of or involved in the systematic manipulation of the publication process.

Wiley and Hindawi regrets that the usual quality checks did not identify these issues before publication and have since put additional measures in place to safeguard research integrity.

We wish to credit our own Research Integrity and Research Publishing teams and anonymous and named external researchers and research integrity experts for contributing to this investigation.

The corresponding author, as the representative of all authors, has been given the opportunity to register their agreement or disagreement to this retraction. We have kept a record of any response received.

### **References**

- [1] S. Liu, "Color Image Landscape Photo Hand-Painted Effect Evaluation with PFA Algorithm," *Advances in Multimedia*, vol. 2021, Article ID 1732919, 9 pages, 2021.

## Research Article

# Color Image Landscape Photo Hand-Painted Effect Evaluation with PFA Algorithm

Shizhang Liu <sup>1,2</sup>

<sup>1</sup>College of Art and Technology (Department), Chengdu College, University of Electronic Science and Technology of China, Chengdu 610000, China

<sup>2</sup>Art College, CITI University of Mongolia, Ulaanbaatar 999097-15141, Mongolia

Correspondence should be addressed to Shizhang Liu; 160108202@stu.cuz.edu.cn

Received 23 August 2021; Accepted 28 October 2021; Published 10 December 2021

Academic Editor: Zhendong Mu

Copyright © 2021 Shizhang Liu. This is an open access article distributed under the Creative Commons Attribution License, which permits unrestricted use, distribution, and reproduction in any medium, provided the original work is properly cited.

With the continuous development of society and economy, diversified presentation and publicity of landscape are becoming more and more popular among the public, such as using color pictures to display multimedia publicity videos or APP, WeChat public accounts, and other new media. There are various ways of expression. Against the limitations of color image landscape, this article introduced the PFA algorithm, during the experiment of hand-painted landscape pictures, the effect of color hand-painted images is evaluated by using the coordination degree of natural target detection scene, and the corresponding image evaluation index values are obtained for effective analysis, and the prediction model is established. The simulation results show that the PFA algorithm is effective and can support the evaluation of the hand-painted effect of color landscape photos.

## 1. Introduction

With the continuous development of the social economy, the presentation and display of the scenery have become the focus of the work of scenic spots and local governments. For landscape publicity, multimedia methods such as color images and publicity videos can be used for publicity through WeChat public accounts, mobile apps, and official homepages [1–4]. There are many ways to acquire color images, which can be fused by imaging tools to form a color image that is visible to the naked eye [5, 6]. For different color image fusion effects, different algorithms can be used for fusion to achieve comprehensive fusion of various bands [7, 8].

The evaluation of image scenery photos can often be divided into subjective and objective evaluations. The so-called subjective evaluation is to judge the quality of the photos based on the user's subjective perception; the

objective evaluation is to use the corresponding objective evaluation model to conduct human simulations to ensure objective and objective evaluation. However, it should be noted that since the human eye is the main receiver, the evaluation based on subjective perception has the advantages of intuition and visibility and can realize the validity of the inspection of image landscape photos [9, 10].

Aiming at the limitations of the effect evaluation of image landscape photos, this paper introduces the PFA algorithm, sorts out the subjective evaluation test indicators of landscape photos, and uses multiple linear regression analysis methods to determine the hand-painted effect parameters of color image landscape photos, determine the influencing factors. The hand-drawn effect experiment of image landscape photos aims to explore the effectiveness of the PFA algorithm.

## 2. PFA Algorithm

For the PFA algorithm, it can be obtained by deriving the bunching of a single point target. Assuming that the rectangular coordinates of a point target in the ground area projected in the oblique plane are  $(x, y)$ , then the time is between the start and the end. The distance is as shown in the following formula:

$$R(t_a) = \sqrt{[R_0(t_a)\cos(\theta(t_a)) - x]^2 + [R_0(t_a)\sin(\theta(t_a)) - y]^2}. \quad (1)$$

$$s(t, t_a) = \text{rect}\left(\frac{t - 2R(t_a)/c}{T_p}\right) \exp\left(j2\pi f_c \left[t - \frac{2R(t_a)}{c}\right] + j\pi\gamma \left[t - \frac{2R(t_a)}{c}\right]^2\right), \quad (2)$$

where  $t$  is the fast time,  $T_p$  is the pulse width, and  $\gamma$  is the distance modulation frequency. When dechirp, the spotlight mode selects the reference distance as  $R_c$ , and the reference

$$s(t, R_c) = \text{rect}\left(\frac{t - 2R_c/c}{T_p + T_s}\right) \exp\left(j2\pi f_c \left[t - \frac{2R_c}{c}\right] + j\pi\gamma \left[t - \frac{2R_c}{c}\right]^2\right), \quad (3)$$

where  $T_s$  represents the maximum value of the difference in echo delay as shown in the following formula:

$$s_{if}(t, t_a) = s(t, t_a) \cdot s^*(t, R_c) = \text{rect}\left(\frac{t - 2R(t_a)/c}{T_p}\right) \cdot \exp\left(j \frac{4\pi[f_c + \gamma(t - 2R_c/c)]}{c} (R(t_a) - R_c)\right) \cdot \exp\left(j \frac{4\pi\gamma}{c^2} (R(t_a) - R_c)^2\right), \quad (4)$$

where  $\exp(j4\pi\gamma/c^2 (R(t_a) - R_c)^2)$  is called the residual video residual term, and the existing method of eliminating residual video phase error (RVP) is used, as shown in Figure 1.

The reference function  $s_{RVP}(f)$  is shown in the following formula:

$$s_{RVP}(f) = \exp\left(-j\pi \frac{f^2}{\gamma}\right), \quad (5)$$

where  $f$  represents the distance frequency. The expression of the echo after eliminating RVP is shown in the following formula:

$$s_{tta}(t, t_a) = \text{rect}\left(\frac{t - 2R(t_a)/c}{T_p}\right) \cdot \exp\left(j \frac{4\pi[f_c + \gamma(t - 2R_c/c)]}{c} (R(t_a) - R_c)\right). \quad (6)$$

**2.1. Simple Color Fusion.** For color fusion, it is the fusion of the color channels of the image, rather than any processing of the image, to achieve the fusion of the three primary colors of R, G, and B.

A large number of studies have shown that red is easy to recognize by the human eye. Therefore, based on this fact,

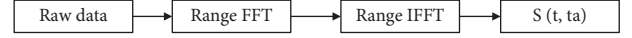


FIGURE 1: Flow chart of eliminating residual video phase error.

The undemodulated echo of the point target can be expressed as shown in the following formula:

echo expression is obtained as shown in the following formula:

the image of the image target can be mapped to the red channel first, so that the background can be easily recognized [11–13]. Since human eyes have different perceptions of the color brightness of monochromatic light, in the image spectrum of the three primary colors, it is easy to think that green is the brightest. Therefore, images containing more

attribute information can be mapped to the green channel. For blue, it can reduce the visual fatigue of the human eye, so it can be followed for a longer period of time.

*2.2. Color Fusion Based on Enhanced Processing and HSV Transformation.* For enhancement processing, it is processed on the basis of the original feature attributes of the image. Its feature is to adjust the human eye's different comfort according to the cold and warm tones of the color, clarify the appropriate color image fusion method, and perform HSV at the same time. The spatial coordinates of color image are transformed to obtain the optimized value.

For ordinary images, it provides a wealth of relevant background information. At the same time, the fusion of hand-drawn photos of color images can make the corresponding images relatively natural. For the image with blurred background, the eigenvalues of the original data of color image are analyzed mainly according to the original data, and the details of the infrared image are relatively clear. Different from the three primary colors of *R*, *G*, and *B*, the HSV model is user-oriented, corresponding to hue, saturation, and brightness. Through reasonable analysis of the three parameters, the corresponding image fusion quality can be improved.

*2.3. Color Fusion Based on Human Visual Characteristics.* For users, the processing and mining of image information are very important, and it is extremely meaningful to use human visual characteristics to perform corresponding image fusion processing. First, the ON and OFF channels are used to enhance the three primary color images to form a neural network again. At the same time, the neural network and the RGB channel mapping are enhanced and post-processed to form a near-natural color hand-drawn image observed by the human eye.

*2.4. Color Fusion Based on YIQ Transform.* For YIQ, *Y* is brightness, and *I* and *Q*, respectively, represent colors. The color vision of the human eye indicates that the human eye can distinguish the color changes of red and blue. Relying on the color fusion of the human eye neural network, the color fusion of the image can be carried out based on YIQ. It can further identify the target and locate [14–16].

### 3. Experimental Design of Hand-Painted Effects of Color Image Landscape Photos

For the experimental analysis of the hand-drawn effect of color image landscape photos, the analysis methods can be divided into subjective and objective aspects. Subjective methods have certain arbitrariness and limitations, but their methods are relatively simple and fast. Therefore, for those with low demand, you can use it directly; the objective evaluation method is to use objective parameters for evaluation, which is necessary.

*3.1. Observers of Subjective Evaluation Experiments.* Set the corresponding number of subjective evaluation observers. The number of subjects in this experiment is 50 people, including 24 girls and 26 boys. During the analysis and evaluation, the students were subjected to a relevant image discrimination test to ensure that they have normal vision and discrimination. It is convenient and clear to distinguish the meaning of the index, mainly from three aspects: target recognition, detailed information, and the background color of the image.

The so-called target recognition is based on the more obvious the target color difference of the image, the more obvious the target, and the higher the recognition effect, efficiency, and accuracy; the detailed information of the image is mainly related to the contrast, edge, and texture of the image; the background color of the image is mainly affected by the color [17, 18].

*3.2. Image of Subjective Evaluation Experiment.* The color hand-drawn images used in the subjective evaluation test mainly include three scenic areas: green, sea and sky, and towns. There are a total of 200 pictures of all the scenic areas.

*3.3. Subjective Evaluation Index.* The subjective evaluation indicators mainly include 2 major categories and 4 secondary categories.

For the same image, the evaluation results of the image hand-drawn effect obtained by different visual tasks are different, according to different image perception quality indicators:

- (1) *Evaluation of the Hand-Painted Effect of Color Image Landscape Photos.* According to the target detection method, the better the target detection, the higher the evaluation score for the hand-painted effect.
- (2) *Evaluation of the Hand-Drawn Effect of Color Image Landscape Photos.* According to the image definition, color coordination, and other indicators, we can quickly understand the image content of hand-painted content and then increase the image evaluation score.

In order to evaluate the single performance of color hand-drawn images, four secondary categories are designed.

*3.3.1. Perceived Contrast.* Perceived contrast is one of the basic characteristics of hand-painted photos. It is mainly to find the degree of easy discovery of the target. It has a greater impact on the quality of the hand-painted effect. If the value is too large or too small, the details of the hand-painted image will be unclear and the image quality will decrease.

*3.3.2. Clarity.* Sharpness is an indicator for users to evaluate the quality of hand-drawn images, reflecting the clarity of the details and textures of the hand-drawn images themselves.

3.3.3. *Color Coordination.* The color coordination is the result of the user's satisfaction according to the color matching and proportion, which is related to the number of colors, the area occupied, and the relative position.

3.3.4. *The Natural Sense of Color.* The naturalness of the color is the contrast degree of the fused hand-drawn image obtained by the corresponding fusion algorithm, so that the color is consistent with the color of the real scene.

3.4. *Subjective Evaluation Experiment Process.* In order to avoid visual fatigue caused by students observing images for a long time, take a break of 5 minutes every 30 minutes and divide the different secondary classifications into different parts. Each student will give a corresponding score for different hand-drawn images.

## 4. Simulation Experiment Results and Data Analysis

First, divide the color image landscape hand-drawn photos in the same landscape range into the same group (including different data processing methods), and standardize the data. The specific calculation can be obtained by the following formula:

$$z_{ij} = \frac{y_{ij} - y_j^{\min}}{y_j^{\max} - y_j^{\min}}. \quad (7)$$

Among them,  $RGB = (R + G + B)/3$  is the original score,  $y_j^{\min}$  and  $y_j^{\max}$  are the minimum and maximum values in the set of data, and  $z_{ij}$  is the transformed score. The scores of 52 observers are converted from the standard 0–1 and then added and averaged to obtain the final scores of the 6 evaluation indicators of the corresponding image. Then, the linear relationship between the 4 single indicators and the regression equation between the composite indicator and the 4 single indicators based on this comprehensive score are analyzed.

Figure 2 shows the four Pearson correlations of the FPA algorithm. It can be seen that TM and S have a strong correlation; CH and CN have a strong correlation.

4.1. *Prediction Model of Comprehensive Perceptual Quality of Plant Background.* The results of TM regression analysis of plant background are shown in Figure 3. At the same time, the TM regression model of plant background can be calculated by the following formula:

$$PQTD = 0.907PCTB + 0.129CH - 0.022(R^2 = 0.958). \quad (8)$$

The SE regression analysis result of plant background is shown in Figure 4. It can be seen that the significance level of the evaluation index CH is less than 0.05, and the specific calculation of the SE regression model of plant background is shown in the following formula:

$$PQSU = 1.044CH - 0.022(R^2 = 0.980). \quad (9)$$

4.2. *Comprehensive Perceived Quality Prediction Model of Haitian Background.* The TM regression analysis result of the sea and sky background is shown in Figure 5, and the TM regression equation of the sea and sky background is shown in the following formula:

$$PQTD = 0.340PCTB + 0.8385S - 0.090(R^2 = 0.846). \quad (10)$$

The results of SE regression analysis of Haitian background are shown in Figure 6.

The SE regression equation of the sea and sky background is shown in the following formula:

$$PQSU = 1.010CH - 0.008(R^2 = 0.985). \quad (11)$$

4.3. *Comprehensive Perceived Quality Prediction Model for Urban Scenes.* The results of TM regression analysis of urban background are shown in Figure 7.

The regression coefficients in model 2 are statistically significant, and there is no multicollinearity problem. The determination coefficient  $R^2$  indicates that PCTB and S can explain 77.7% of the TM changes. The TM regression equation of the urban scene is shown in the following formula:

$$PQTD = 0.601PCTB + 0.440S - 0.027(R^2 = 0.777). \quad (12)$$

The SE regression analysis results of the urban background are shown in Figure 8, and the TM regression equation of the urban scene is shown in the following formula:

$$PQSU = 0.885CH + 0.150S - 0.024(R^2 = 0.990). \quad (13)$$

From the results of the above simulation experiments, the analysis of the color coordination of the color hand-drawn images shows that PFA is effective. In addition, in different landscape environments, this article differs from traditional methods in plants, sea, and sky scenes and basically consistent with traditional results in urban scenes.

From the analysis results of the three types of scenes (Figure 8), it can be seen that the target background perception contrast occupies a large proportion in the image perception quality TM prediction model based on target detection, and the definition also occupies a certain proportion, but the impact is small.

4.4. *Comparison and Evaluation of Color Hand-Drawn Image and Source Image.* At present, there is no ideal evaluation index between the color hand-drawn image and the source gray image. Therefore, this section compares the grayscale information of the color hand-drawn image with the source grayscale image.

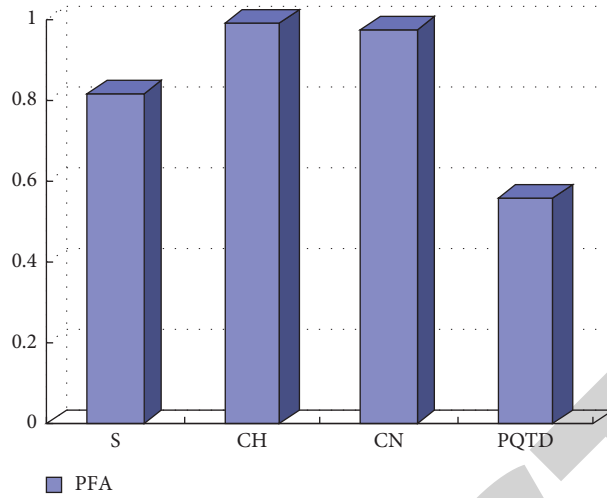


FIGURE 2: Pearson correlation coefficient of the PFA algorithm.

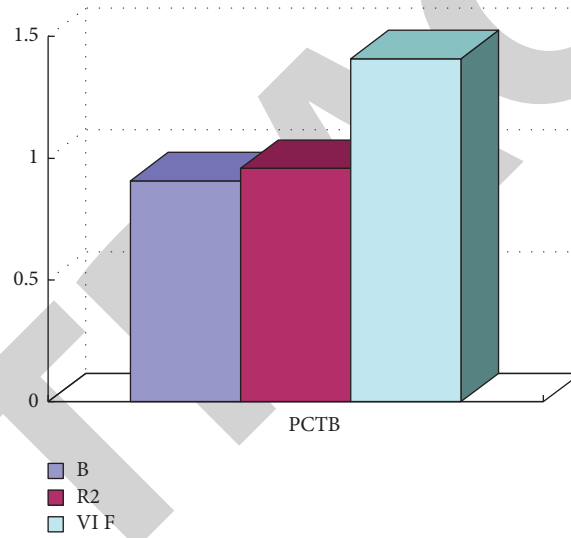


FIGURE 3: TM regression model of plant background.

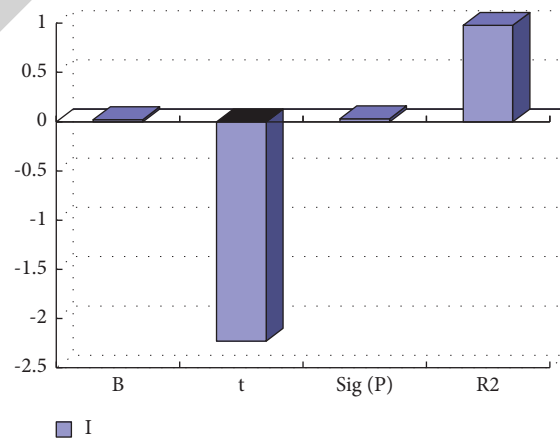


FIGURE 4: The regression model of plant background for SE.

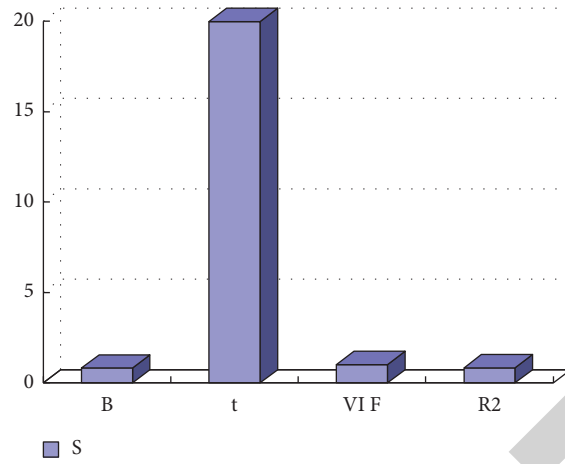


FIGURE 5: The regression model of Haitian background for TM.

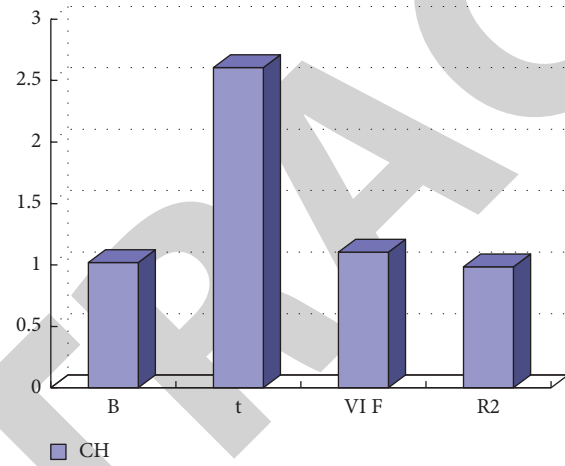


FIGURE 6: The regression model of Haitian background for SE.

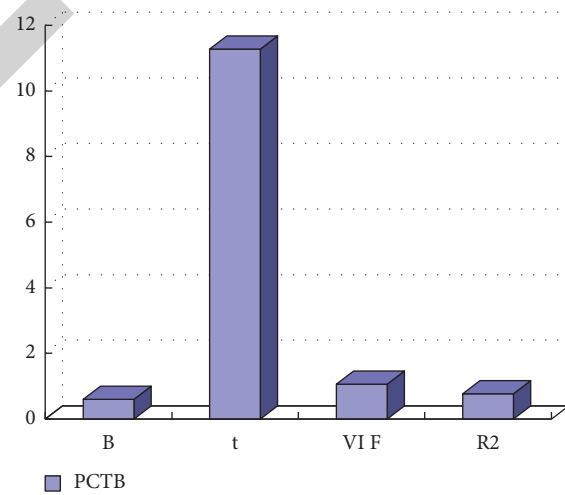


FIGURE 7: Regression model for TM in urban context.

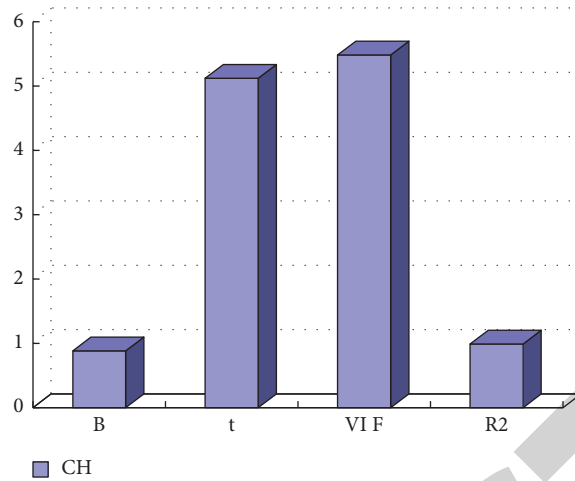


FIGURE 8: The regression model of urban context against SE.

TABLE 1: Comparison of gray information between source image and YIQ transformed color hand-drawn image.

	Entropy	Average target background contrast	Roughness
Visible light image	7.03	0.33	9.93
Midwave infrared image	6.85	5.22	5.72
Longwave infrared image	7.25	2.03	7.83
Brightness part of fusion result 1	6.85	3.23	8.41
Brightness part of fusion result 2	7.74	5.14	9.84
Brightness part of fusion result 3	7.01	1.34	8.01
Brightness part of fusion result 4	6.44	0.89	7.91

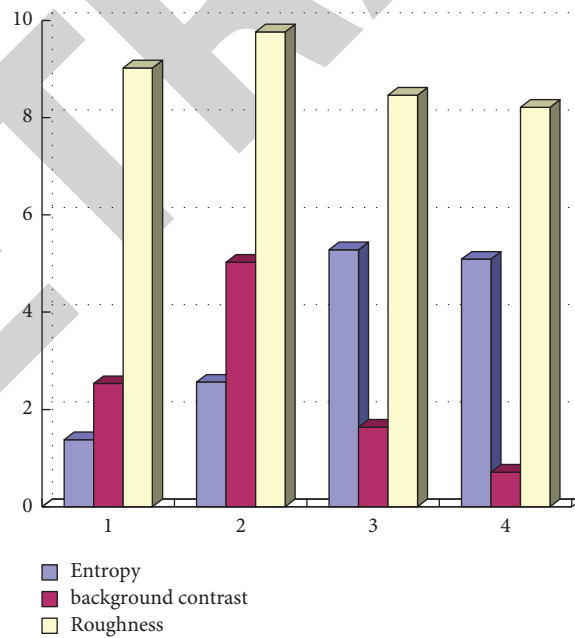


FIGURE 9: Comparison of the source image and the average weighted result.



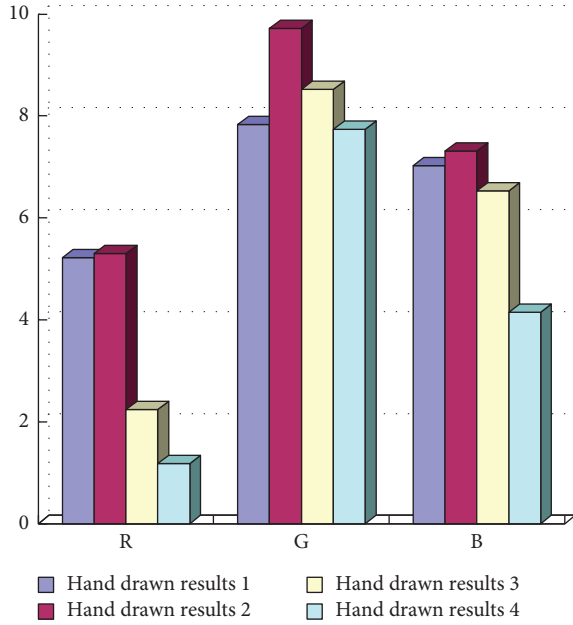


FIGURE 10: Comparison between color fusion results.

**4.4.1. Evaluation Method Based on YIQ Transformation.** YIQ transform can well separate the brightness part and the color part of a color image. The specific conversion process from RGB color space to YIQ color space is shown in the following formula:

$$\begin{bmatrix} Y \\ I \\ Q \end{bmatrix} = \begin{bmatrix} 0.299 & 0.587 & 0.114 \\ 0.596 & -0.275 & -0.321 \\ 0.212 & -0.523 & -0.311 \end{bmatrix} \begin{bmatrix} R \\ G \\ B \end{bmatrix}. \quad (14)$$

Therefore, it can be obtained as shown in the following formula:

$$Y = 0.299R + 0.587G + 0.114B. \quad (15)$$

Use YIQ transform to separate the brightness information of the four color hand-drawn images in Figure 1, and compare them objectively with the source image. The parameters are shown in Table 1. The fusion results 1, 2, 3, and 4 in Table 1 are  $a$ ,  $b$ ,  $c$ , and  $d$  in Figure 1, respectively.

**4.4.2. Evaluation Method Based on Weighted Average.** The  $R$ ,  $G$ , and  $B$  channels of the color hand-drawn image are processed by weighted average, and the processed results are compared objectively with the source image. The specific processing process is shown in the following formula:

$$RGB = \frac{(R + G + B)}{3}. \quad (16)$$

RGB1, RGB2, RGB3, and RGB4 in Figure 9, respectively, represent the images after the weighted average of the  $R$ ,  $G$ , and  $B$  channels of the 4 color hand-drawn images.

It can be seen from the results that the entropy of the four fusion results is smaller than that of the source image, and the amount of information is lost to varying degrees; the average

target background contrast of RGB2 is similar to that of mid-wave infrared, and the target is more obvious. The contrast of RGB1 and LWIR is similar, RGB3 and RGB4 are between visible light and LWIR, and the target is not obvious; the roughness of RGB2 is close to the visible light image, and the details are richer.

#### 4.5. Evaluation Method among Color Hand-Drawn Images.

The average target background contrast of the  $R$  component is calculated to compare whether the target is obvious, the roughness of the  $G$  component is calculated to indicate the amount of detailed information, and the entropy of the  $B$  component is calculated to indicate whether the background is rich.

The data in the  $R$ ,  $G$ , and  $B$  columns in Figure 10, respectively, represent the average target background contrast, roughness, and entropy of the  $R$ ,  $G$ , and  $B$  three channels. Considering the contrast, roughness, and entropy, each component of the hand-drawn result 2 is larger than the other three, and the effect is ideal.

## 5. Conclusions

The hand-painting of color images and landscape photos is one of the important ways and means to publicize landscapes and local recommendations. Therefore, more and more attention is paid to the effect and quality of its effects. In view of the existing limitations, this paper introduces the PFA algorithm, constructs a color image landscape photo effect evaluation model by combing the corresponding evaluation indicators, uses 50 students to evaluate the hand-painted effect experiment, and analyzes it through subjective and objective aspects. The simulation results show that the PFA algorithm is effective and can support the evaluation of the hand-painted effect of color image landscape photos.

## Data Availability

The data used to support the findings of this study are available upon request to the author.

## Conflicts of Interest

The author declares that there are no conflicts of interest.

## References

- [1] D.-J. Lee and D. Y. Kim, "Paper-based, hand-painted strain sensor based on ITO nanoparticle channels for human motion monitoring," *IEEE Access*, vol. 7, no. 3, pp. 77200–77207, 2019.
- [2] E. I. Wolfe and C. Barker, "Extreme canvas: hand-painted movie posters from Ghana," *Toxicology Letters*, vol. 238, no. 2, pp. 219–225, 2015.
- [3] N. Santos, B. Rodrigues, V. Otero, and M. Vilarigues, "Defining the first preventive conservation guidelines for hand-painted magic lantern glass slides," *Conservar Património*, vol. 7, no. 3, pp. 68–73, 2021.
- [4] B. V. Wesemael, J. Poesen, T. D. Figueiredo, and G. Govers, "Surface roughness evolution of soils containing rock fragments," *Earth Surface Processes and Landforms*, vol. 21, no. 5, pp. 399–411, 2015.

- [5] S. Mark, F. Alexandra, K. Balázs, S. Dénes, B. András, and H. Gábor, "How realistic are painted lightnings? Quantitative comparison of the morphology of painted and real lightnings: a psychophysical approach," *Proceedings of the Royal Society A Mathematical Physical & Engineering Sciences*, vol. 474, no. 2214, pp. 2017–2024, 2018.
- [6] S. Nam, Y. Kim, and Y. Lim, "Materialization of interactive stereoscopic artwork based on hand-painted images," *Multimedia Tools and Applications*, vol. 77, no. 1, pp. 149–163, 2018.
- [7] K. Ake, T. Ogura, Y. Kaneko, and G. S. A. Rasmussen, "Automated photogrammetric method to identify individual painted dogs (*Lycaon pictus*)," *Zoology and Ecology*, vol. 29, no. 2, pp. 103–108, 2019.
- [8] D. Zou and C. Wang, "Design hand drawing expression techniques under the background of informatization," *Journal of Physics: Conference Series*, vol. 1744, no. 3, pp. 32016–32028, 2021.
- [9] S. Bottura-Scardina, A. Brunetti, C. Bottaini, and C. Migue, "On the use of hand-held X-ray fluorescence spectroscopy coupled to Monte Carlo simulations for the depth assessment of painted objects: the case study of a sixteenth-century illuminated printed book," *The European Physical Journal Plus*, vol. 136, no. 3, pp. 1–19, 2021.
- [10] I. A. Matveev, A. B. Murynin, and A. N. Trekin, "Method for detecting cars in aerospace photos," *Pattern Recognition and Image Analysis*, vol. 25, no. 4, pp. 669–673, 2015.
- [11] A. V. Buravsky, E. V. Ba Ranov, E. V. Baranov, S. I. Tretyak, and M. K. Nedzved, "Evaluation of effect of local light-emitting diode phototherapy on experimental wounds," *Novosti Khirurgii*, vol. 23, no. 6, pp. 601–611, 2015.
- [12] H. Asai, K. Kojima, S. F. Chichibu, and K. Fukuda, "Theoretical analysis of photo-recycling effect on external quantum efficiency considering spatial carrier dynamics," *Japanese Journal of Applied Physics*, vol. 59, no. 2, pp. 456–462, 2019.
- [13] R. P. D. Souza, A. Lima, O. Pezoti, V. Slusarski-Santana, M. Gimenes, and N. R. C. Fernandes-Machado, "Photodegradation of sugarcane vinasse: evaluation of the effect of vinasse pre-treatment and the crystalline phase of  $\text{TiO}_2$ ," *Acta Scientiarum Technology*, vol. 38, no. 2, pp. 89–94, 2016.
- [14] C. Uslan, N. D. İşleyen, Y. Öztürk et al., "A novel of PEG-conjugated phthalocyanine and evaluation of its photocytotoxicity and antibacterial properties for photodynamic therapy," *Journal of Porphyrins and Phthalocyanines*, vol. 5, no. 2, pp. 1–15, 2018.
- [15] B. Thomas, A. A. Prasad, and S. M. Vithiya, "Evaluation of antioxidant, antibacterial and photo catalytic effect of silver nanoparticles from methanolic extract of coleus vettiveroids—an endemic species," *Journal of Nanostructures*, vol. 8, no. 2, pp. 179–190, 2018.
- [16] D. A. Mochi, A. C. Monteiro, R. C. L. R. Pietro, M. A. Corrêa, and J. C. Barbosa, "Compatibility of metarhizium anisopliae with liposoluble photoprotectants and protective effect evaluation against solar radiation," *Bioscience Journal*, vol. 33, no. 4, pp. 1028–1037, 2017.
- [17] S. M. Hamed, M. P. Raut, S. R. P. Jaffé, and P. C. Wright, "Evaluation of the effect of aerobic–anaerobic conditions on photohydrogen and chlorophyll a production by environmental Egyptian cyanobacterial and green algal species," *International Journal of Hydrogen Energy*, vol. 42, no. 10, pp. 6567–6577, 2017.
- [18] G. Bitencourt, L. J. Motta, D. Silva et al., "Evaluation of the preventive effect of photobiomodulation on orofacial discomfort in dental procedures: a randomized-controlled, crossover study and clinical trial," *Photobiomodulation Photomedicine and Laser Surgery*, vol. 39, no. 1, pp. 564–573, 2020.